Indonesian Journal of Applied Research IJAR

THE EXPERIMENTAL OF IMPACT OF ADDITIONAL MAGNETIC FIELDS AND NITROGEN PRESSURE ON OLIVE OIL DROPLET COMBUSTION

Volume 4 Issue 1
(April 2023)
e-ISSN 2722-6395
doi: 10.30997/ijar.v4i1.280

Dony Perdana[1]

[1] *Department of Mechanical Engineering, Universitas Maarif Hasyim Latif, Sidoarjo, Indonesia*

ARTICLE INFO

Article history:
Received: 09-01-2023
Revised version received: 16-01-2023
Accepted: 29-03-2023
Available online: 02-04-2023

Keywords:
Flame characteristic; Attracting magnetic field; Olive oil; Droplet combustion; Various N_2 pressure.

How to Cite:
Perdana, D. (2023). THE EXPERIMENTAL OF IMPACT OF ADDITIONAL MAGNETIC FIELDS AND NITROGEN PRESSURE ON OLIVE OIL DROPLET COMBUSTION. *Indonesian Journal of Applied Research (IJAR)*, *4*(1), 1-10. https://doi.org/10.30997/ijar.v4i1.280

Corresponding Author:
Dony Perdana
dony_perdana@dosen.umaha.ac.id

ABSTRACT

This experiment studies the impact of a magnetic field of attraction and various nitrogen pressures in the combustion chamber on the characteristics of the flame. To replace depleted fossil fuels, the usage of vegetable oil is crucial. This research aims to probe the droplet combustion of olive oil on evolution, temperature, height, and ignition delay. The camera's high speed is 120 frames per second front-facing camera records the process from the start flamed until it has extinguished. A droplet of olive oil is placed on a type K thermocouple between two magnet rods in a nitrogen-pressurized chamber—three variations of nitrogen pressure in the combustion chamber, which included 0.5, 1, and 1.5 bar. The results found that the nitrogen pressure of 0.5 bar led to evolution, and the flame stability was more stable. Moreover, the highest temperature and flame delay was shorter than the pressures of 1 bar and 1.5 bar. At a pressure of 0.5 bar, the flame evolution was 1200 milliseconds, the maximum temperature was 741 °C, and the ignition delay of 4506 milliseconds was shorter than the other two pressures. That occurred due to high nitrogen pressure inhibiting the collision reaction of the olive oil fuel vapor with air. Meanwhile, adding an attraction magnetic field can centralize oxygen and fuel molecules in the area of the reaction zone, resulting in rapid combustion and a shorter flame delay change.

1. INTRODUCTION

Population, economic activity, industry, and transportation increase, causing the need for energy derived from fossil fuels. In contrast, oil and coal reserves are diminishing yearly. Biomass is a high energy potential vital in scientific studies, especially renewable energy (Hamedani et al., 2018). Diverse types of biomass include vegetable oil, municipal solid waste, green waste, and agricultural waste (Anifantis et al., 2017). One of the biofuels derived from vegetable oil is olive oil, which contains 10-11% oxygen and a lower volumetric heating value (approximately 12%) than diesel. In addition, various types of biomass have been studied severally, including pellets (Shan et al., 2017), pin chips (Serrano et al., 2013), and olive cake (Koukouch et al., 2017). However, direct use causes significant problems, including filter blockage, injection pump damage, and carbon deposits on engine components such as the combustion chamber walls, cylinder heads, and injector nozzles (Shah & Ganesh, 2018). Among the proposed solutions are the following: altering the combustion chamber, exhaust gas recirculation, preheating vegetable oil, and mixing vegetable oil with diesel in varying measures.

Several studies have reported on combustion with olive oil and its derivatives. The diesel engine using olive oil fuel shows performance suitability by adjusting five rotation speeds (650 rpm, 570 rpm, 490 rpm, 410, 320 rpm, and 240 rpm), increasing the torque by 8.43% and power of 28.57 % greater than diesel. At low operating cycles, the specific energy consumption was 12.8% and 30% less than diesel, respectively (Volpato et al., 2012). The experimental study of diesel engine combustion characteristics and pollutant emissions utilizes olive mill wastewater (OMWW). Compared to B20 under high-load conditions, B10 was shown to have lower emissions for UHC (12%), PM (12%), and CO (26%). B10, under moderate load conditions, was found to reduce the content of air particles, among them a PM (55%) and CO (65%), compared to B30. Furthermore, using a mixture of B20 and B30, the BTE produced is less than diesel. On the contrary, B10 makes higher BTE than diesel (Hadhoum et al., 2021). We are examining the effect of olive oil-pomace biodiesel blended with diesel on a Perkins AD 3-152 direct injection diesel engine compared to diesel. If biodiesel has used directly, the power produced is reduced by 5.6%, and fuel consumption increases by 7% (López et al., 2014). Another study examined the performances and pollutant emissions characteristic of a compression ignition engine operating varying loads blended with olive oil biodiesel and diesel. NOx levels are slightly more significant for the mix than diesel by all loads. Because of the presence of inherent oxygen in fuel, the mixture is. Increasing the combustion rates causes an increase in the temperature of the cylinder (Sree et al., 2017).

Besides the previously cited technique, magnetic ionization at fuels is a new technique that researchers have yet to study many. Most liquid fuels are composed of hydrocarbons with significant tensile forces, allowing them to form pseudo compounds. The magnetic fields benefit fuel during combustion (Wahhab et al., 2017) because they can change the fuel's physicochemical properties (Espinosa et al., 2016). Researchers have found that adding a magnet alters the flame's behavior through various measurement techniques (Perdana et al., 2021). A magnetic field shows a significant change in the structures of the flame (Perdana et al., 2020) and variations in temperature (Perdana et al., 2022). The Magnetic field impact on vehicles can decrease fuel consumption and pollution emission. The magnets lowered on a percentage at CO, HC, and NOx gas components (Patel et al., 2014). The permanent magnetic fields at the fuel lines can enhance fuel characteristics by aligning and guiding hydrocarbon molecules for improved fuel atomization, reducing vehicle pollutant emissions (Jain & Deshmukh, 2012). A magnetic field decreases the viscosity of the HC molecule, improving atomization, increasing BTE, and making it more economical (Chaware, 2015).

According to the explanation above, all researchers only researched the performance of internal combustion engines. However, the flame behavior that plays a vital role in combustion stability has yet to be studied widely. The impact of a magnetic field and different nitrogen pressures in a pressurized combustion chamber on the droplet combustion of olive oil as an alternative fuel should receive special attention. Crucial to research the impact of olive oils as fuel on combustion in the combustion chamber, particularly equipment used in the combustion chamber of power plants during long-term operation.

2. METHODS

2.1. Fatty Acids Composition and Physico-Chemical Properties of Olive Oil

Olive oil is a vegetable oil obtained from olives, derived from olive trees that thrive on the Mediterranean continent. Straight olive oil was tested to investigate the effect of natural oil fatty acid composition on droplet combustion. The Olive oil was obtained as commercially available edible oils for domestic use, with the physical-chemical properties and fatty acid composition shown in Table 1-2. The physical properties of olive oil can be seen through density, viscosity, flash point, fire point, and heating value, as depicted the Table 1.

Table 1 The physical properties of olive oil

Vegetable oil	Physical properties			References
Olive oil	Density (g/cm^3)	15 °C	0.917	(Mawatari et al., 2013)
	Kinematic viscosity (mm^2/s)	40 °C	38.7	
		100 °C	8.28	
	Flash Point (°C)		285	Kumar et al., 2014)
	Fire Point (°C)		310	
	Heat of Combustion $\Delta H°_C$ (kJ/g)		43.45	(Villot et al., 2019)

Vegetable oils contain saturated fatty acids, unsaturated fatty acids, and glycerol. Fatty acids comprise straight and long hydrocarbon chains containing 12 to 24 carbon atoms. Olive oil has the highest unsaturated fatty acid content than saturated fatty acids was determined using gas chromatography (GC). Mainly composed of unsaturated fatty acids in olive oil are oleic and linoleic acids, around 72.77% and 9.47%, respectively. Meanwhile, saturated fatty acids, namely palmitic and stearic acid, were 12.09% and 3.01%, respectively. The fatty acid composition is shown in Table 2.

Table 2 The chemical properties of olive oil

Fatty acid		Structure	Value (%)	References
Satured fatty acid	Myristic	C14:0	0.01	(Guo et al., 2018)
	Palmitoleic	C16:1	1.15	
	Palmitic	C16:1	12.09	
	Margaroleic	C17:1	0.1	
	Margaric	C17:0	0.05	

	Stearic	C18:0	3.01
Unsatured fatty acid	Oleic	C18:1	72.77
	Linoleic	C18:2	9.47
	Linolenic	C18:3	0.6
	Arachidic	C20:0	0.36
	Eicosenoic	C20:1	0.23
	Behenic	C22:0	0.11
	Lignoceric	C24:0	0.05

2.2. Experimental Apparatus

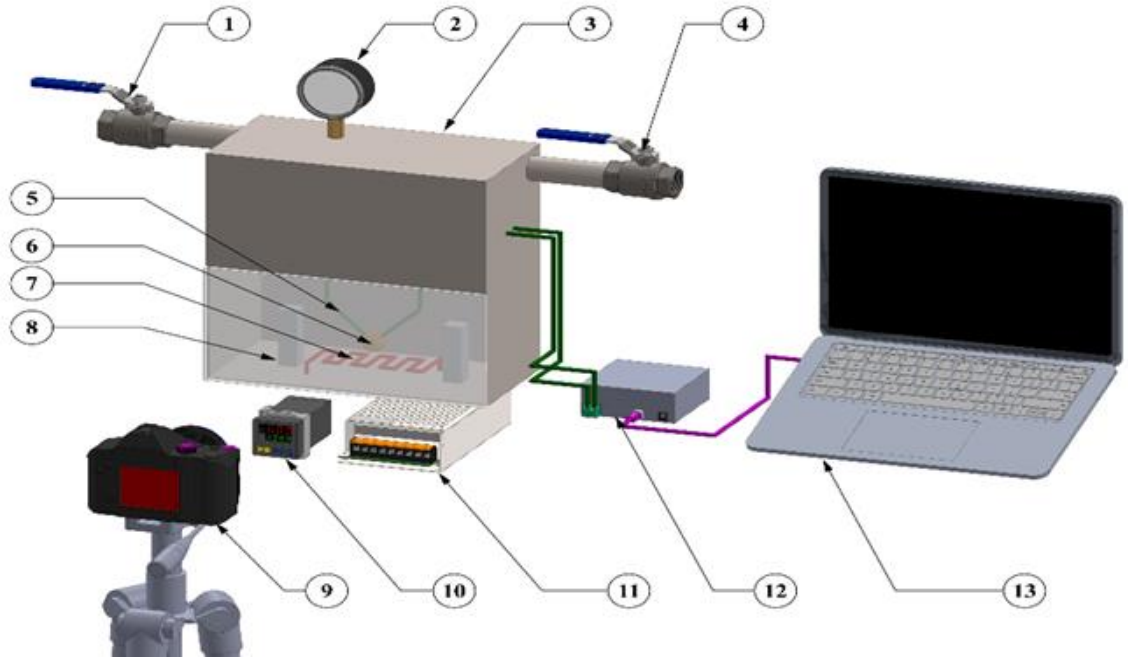

Figure 1 Experimental apparatus: (1) air intake valve; (2) pressure gauge; (3) pressure chamber; (4) n_2 intake valve; (5) thermocouple; (6) droplet; (7) electrical heater; (8) permanent magnet; (9) high-speed camera; (10) temperature controller; (11) power supply; (12) data logger; (13) laptop.

The study has conducted using the experimental apparatus depicted schematically in Figure 1. Olive oil droplets were attached to a 0.1 mm-diameter Pt/Rh13% thermocouple junction of type K. The flame utilizes a Ni-Cr electrics coil heater, wire resistance 1.02 with an electric heater as a 5 A electric current with a 12 V DC power source. A maintained droplet diameter was approximately 0.3 mm, and gas nitrogen (N_2) in the combustion chamber was correspondingly 0.5, 1, and 1.5 bar at various pressure. As shown in Figure 2, the droplets generated on the thermocouple put a 10 mm gap between two neodymium permanent magnet rods. A 40 x 25 x 10 (mm) nickel-plated N45-grade magnet with a magnetic field intensity of 11000 gausses. The magnetic bar has connected to an aluminum plate stand with bolts and nuts for simple removal and installation. That repeated for all examples of measurement ten times.

2.3. Data Acquisition

A Fuji ZR high-speed camera capable of 120 fps captured that image of the formed flame until extinguished. A type K thermocouple connects to the data logger by recording the temperature from when ignited until extinguished. The data collected in this study include evolution, temperature, height, and flame ignition delay. The data retrieval results are then processed using a free video to JPG and Image J converter and converted into several frames. An evolution, height, and flame delay were measured using Corel Draw.

2.4. Position of Magnetic Field

Figure 2 The position of magnetic fields in the north (N) and south (S)

3. RESULTS AND DISCUSSION

3.1. Results

3.1.1. *Evolution and Flame shape from Various N_2 Pressures*

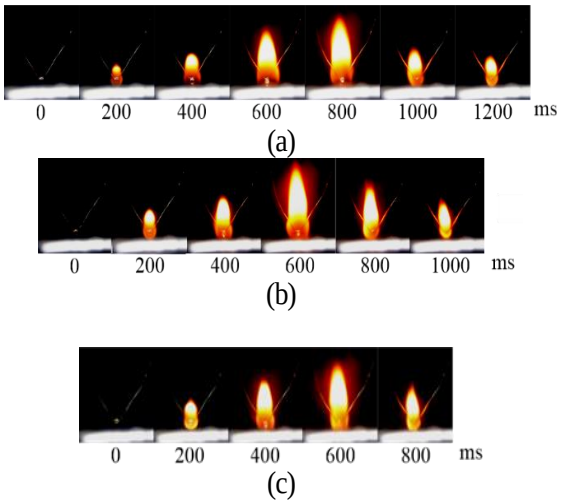

Figure 3 Evolution And Flame Shape Towards Evolution Time At N_2 Pressures; (A) 0.5 Bar, (B) 1 Bar, And (C) 1.5 Bar

Figures 3a-3c show the evolution and flame shape of the attraction magnetic field at varying N_2 pressures. The flame duration values for the N_2 pressure variations of 0.5, 1, and 1.5 bar were 1200 milliseconds (ms), 1000 ms, and 800 ms, respectively. The pressure of N_2 influences the evolution and shape of the flame, as illustrated in Figure 3a, where the flame is slightly broader or fatter than in Figure 3b-3c. That occurred due to the explosion created by

the olive oil's height water content. Various nitrogen pressures affect the flame time. The higher the nitrogen gas pressure, the shorter the flame time. This happens because the value of density is inversely proportional to pressure. The higher the pressure, the lower the density.

3.1.2. *Temperature and Flame Evolution Time from Various N_2 Pressure*

Figure 4 shows the temperature for the time of evolution, a magnetic field of attraction, and variations in N_2 pressure in the combustion chamber. Before the extinguished flame, the temperature increased, then decreased in response to three variations in N_2 pressure. At an N_2 pressure of 0.5 bar at 1000 ms, the most significant temperature was 741 °C, followed by 1 bar and 0.5 bar at 634.25 °C and 539 °C, respectively. The lowest temperature occurred as the flame began to form at 465.75 °C at an N_2 pressure of 1.5 bar, followed by 1 bar and 0.5 bar, corresponding to 476.75 °C and 500.25 °C, respectively.

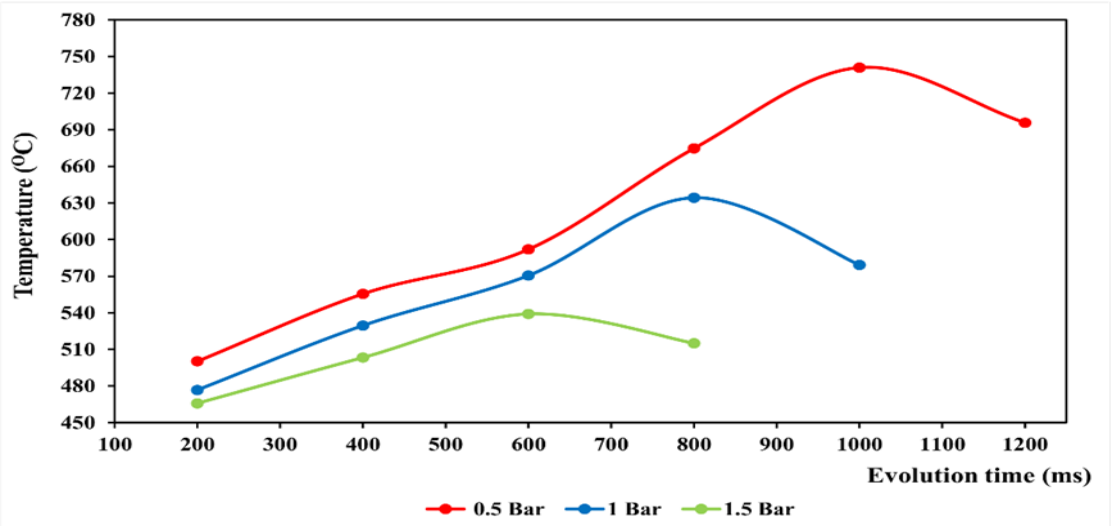

Figure 4 Flame Temperature Versus Evolution Time The Variations In Nitrogen Pressure

3.1.3. *Temperature and Flame Evolution Time from Various N_2 Pressure*

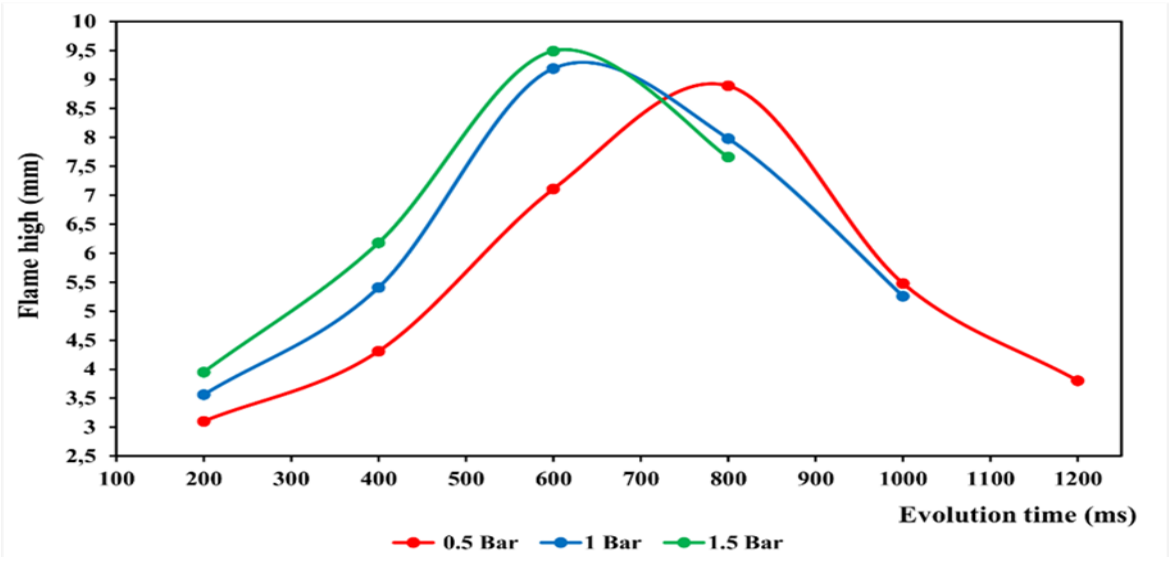

Figure 5 Flame Height Versus Evolution Time Variations In Nitrogen Pressure

Figure 5 shows the flame height for the time of evolution, a magnetic field of attraction, and variations in N_2 pressure in the combustion chamber. At pressure variations of 0.5 bar, 1 bar, and 1.5, the height of the flame increased until it reached its maximum peak, at which point it decreased until it burned out. The highest flame produced was 9.49 mm at 600 ms at a pressure of 1.5 bar N_2, followed by 9.19 mm at 1 bar and 8.89 mm at 800 ms at a pressure of 0.5 bar. A small nitrogen pressure produces the lowest flame height.

3.1.4. *Ignition Delay Time of Various N_2 Pressure*

The N2 pressure of 1.5 bar produced the longest flame delay time of 6732 ms, followed by 1 bar of 5540 ms. Figure 6 depicts that the quickest time for igniting a flame at an N2 pressure of 0.5 bar was 4506 milliseconds. As shown in Figure 6, the flame delay time trend decreases by adding various nitrogen pressures. In general, there are three groups of flame delay times, the first is 0.5 bar pressure, the second is 1 bar, and the last is 1.5 bar. Nitrogen pressure of 0.5 bar produces the shortest flame delay time, compared to 1 bar and 1.5 bar. Nitrogen pressure of 1 and 1.5 bar inhibits the atomization process by reducing the formation of the mixture so that the ignition delay time is longer.

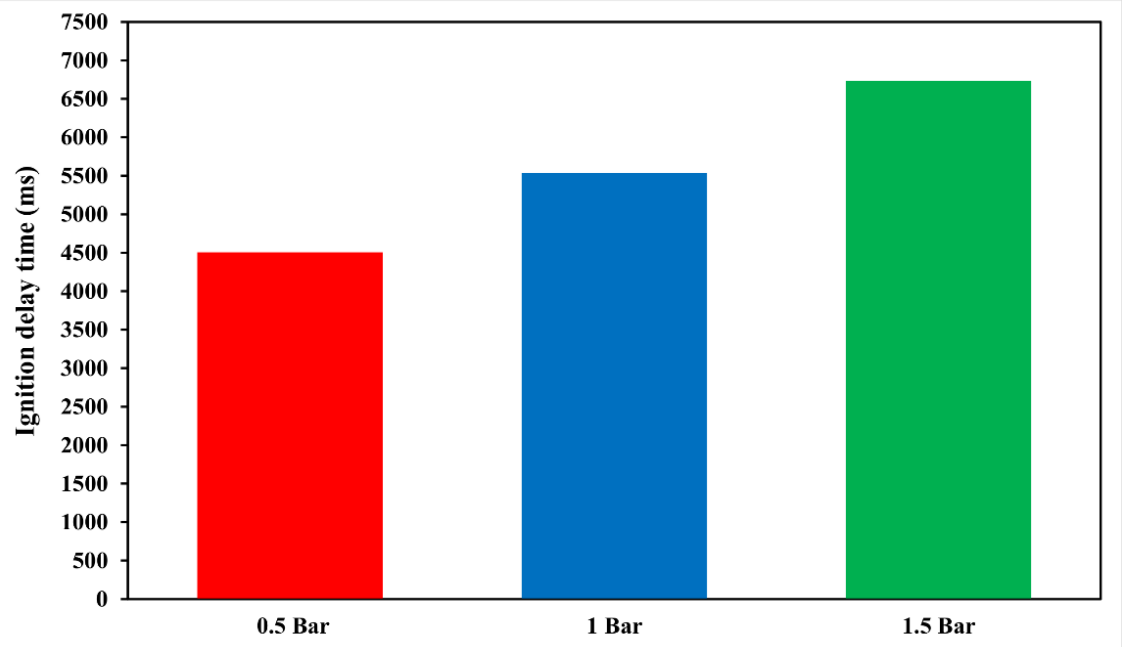

Figure 6 Flame Delay Time Versus Variations Of Nitrogen Pressures

3.2. Discussion

The high N_2 pressure accelerates water evaporation from the oil before ignition, shortening the flame's duration. Second, the density is inversely proportional to the N_2 pressure. As pressure and temperature increase, the density decreases. This difference in flame height caused by a magnetic field of attraction affects the combustion to complete. That occurs due to the accelerated electron spins caused by a magnetic field of attraction on the electrons in the reactants. With low N_2 pressure, the magnetic field has a more significant influence, making the flame steadier. A strong magnetic field pulls O_2 across on flame while H_2O is pumped as a heat resource (Perdana et al., 2020).

The higher the N_2 pressure addition in the combustion chamber, the lower the laminar combustion speed and convection heat. That reduces heat release and increases heat capacity on the unburned gas mixtures, lowering the flame temperature. The trend of temperature

changes with varying N_2 pressure parallels the movement of the laminar flame speed changes. That is due to the flame's speed indicating the combustion reaction rate. Although a magnetic field of attraction increased the flame temperature, previous research suggested magnetic fields lowered the temperature, and the more significant rise in N_2 pressure resulted in a smaller decrease in temperature. That may be because some heat evaporates the olive oil, which is more challenging due to the larger molecular attractive forces resulting from higher polarity. At an N_2 pressure of 0.5 bar, the increase in temperature was more prominent, indicating that a magnetic field of attraction helps to stabilize the combustion. The most significant temperature of the droplets happens near the end of the combustion process, as the droplets have consumed. The high flame temperature of olive oil combustion indicates the amount of power it creates.

This height difference was possible due to the pressure differential of N_2. The greater the pressures of N_2, the faster fuel evaporation, resulting in a quicker combustion process when it diffuses into the air and a shorter flame height in the middle of the combustion phase. That is because evaporation at the droplet surface produces more vapor. Furthermore, the size of the flame decreased drastically after reaching its optimum height until on flame was extinct. The increasing combustion rate of by combustible mixture leaves fuel vapor around droplets. This difference in flame height by the attraction magnetic field affects the combustion to complete. A magnetic field of attraction attracts O_2 from the surrounding air, accelerating the combustion reaction process with fuel. That indicates a flame with a higher nitrogen pressure was likely less stable due to its high stretch. The magnetic field significantly impacts lowering flame height, as it creates energetic electrons increasing reaction rates that can compensate for the diffusion rate (Perdana et al., 2022). That occurs because a magnetic field of attraction affects the flow rate of O_2, which causes convection around the flame; therefore, oxygen flows to the bottom of on flames on both sides due to of attractive force of the magnetic field. This flow increases the concentration of oxygen and fuel molecules in the region of the reaction zone, resulting in a shorter, more reactive combustion and a very short flame height (Perdana et al., 2020) (see Figure 3).

The pressure of N_2 is high, causing a longer flame delay time; this disturbs the development of a flame due to the absence of outside air in the combustion reaction and prevents the collision of the reaction material. As a result of mixing fuel with air, the combustion process could be better. In contrast, when the N_2 pressure is low, the attractive magnetic field increases the atomization process and the blend's formation, reducing flame delay time. This shorter evaporation process leads to fuel and oxidizer diffusing in a more concentrated area. The shortest flame delay occurs because, initially, the magnetic field generates an electromagnetic force that interferes with the electrons in olive oil. As a result, the activation energy required to react with the fuel and oxygen decreased, resulting in relatively rapid burning. Second, the magnetic field facilitates the entry of O_2 and H_2O particles through droplets, resulting in the collision of larger fuel particles, which weakens the bonds between fuel molecules. The weakened chemical bonds in the fuel will increase the distance between molecules, making it easier for O_2 to react with the fuel more quickly. In addition, the magnetic field can reduce viscosity and the surface tension on fuel (Oommen & Kumar, 2020). Decreasing the viscosity of fuel makes molecules more energetic, thus accelerating the nucleation process in the droplet.

4. CONCLUSION

Observation of combustion at the beginning of the flame has formed until extinguished in a pressurized combustion chamber. From this study, several findings were obtained, including High N_2 pressure inhibits the evaporation of olive oil for a longer time, causing diffusion of fuel and oxidizer across a larger surface area; this results in more large flames. N_2

is the primary factor that reduces laminar combustion speed and thermal diffusion. The magnetic field of attraction produces optimal distances between hydrocarbon molecules, which causes them to react more reactively with oxygen, making them more flammable.

ACKNOWLEDGMENT

Special thanks to Imam Basyori, for collecting the experimental data. Maarif Hasyim Latif University, Sidoarjo, funded this study.

REFERENCES

Anifantis, A. S., Colantoni, A., & Pascuzzi, S. (2017). Thermal energy assessment of a small scale photovoltaic, hydrogen and geothermal stand-alone system for greenhouse heating. *Renewable Energy*, *103*, 115–127. https://doi.org/10.1016/j.renene.2016.11.031

Chaware, K. (2015). Review on effect of fuel magnetism by varying intensity on performance and emission of single cylinder four stroke diesel engine. *International Journal of Engineering Research and General Science*, *3*(1), 1174–1178. http://pnrsolution.org/Datacenter/Vol3/Issue1/155.pdf

Espinosa, E. A. M., Rodríguez, R. P., Sierens, R., & Verhelst, S. (2016). Emulsification of waste cooking oils and fatty acid distillates as diesel engine fuels: An attractive alternative. *International Journal of Sustainable Energy Planning and Management*, *9*, 3–16. https://doi.org/10.5278/ijsepm.2016.9.2

Guo, Z., Jia, X., Zheng, Z., Lu, X., Zheng, Y., Zheng, B., et al. (2018). Chemical composition and nutritional function of olive (Olea europaea L.): a review. *Phytochemistry Reviews*, *17*(5), 1091–1110. https://doi.org/10.1007/s11101-017-9526-0

Hadhoum, L., Aklouche, F. Z., Loubar, K., & Tazerout, M. (2021). Experimental investigation of performance, emission and combustion characteristics of olive mill wastewater biofuel blends fuelled CI engine. *Fuel*, *291*, 120199. https://doi.org/10.1016/j.fuel.2021.120199

Hamedani, S. R., Villarini, M., Colantoni, A., Moretti, M., & Bocci, E. (2018). Life cycle performance of hydrogen production via agro-industrial residue gasification-a small scale power plant study. *Energies*, *11*(3), 675. https://doi.org/10.3390/en11030675

Jain, S., & Deshmukh, S. (2012). Experimental investigation of magnetic fuel conditioner (M.F.C) in I.C. engine. *IOSR Journal of Engineering (IOSRJEN)*, *2*(7), 27–31. https://doi.org/10.9790/3021-02712731

Koukouch, A., Idlimam, A., Asbik, M., Sarh, B., Izrar, B., Bostyn, S., et al. (2017). Experimental determination of the effective moisture diffusivity and activation energy during convective solar drying of olive pomace waste. *Renewable Energy*, *101*, 565–574. https://doi.org/10.1016/j.renene.2016.09.006

Kumar, S. S., Iruthayarajan, M. W., & Bakrutheen, M. (2014). Analysis of vegetable liquid insulating medium for applications in high voltage transformers. *Proceedings International Conference on Science Engineering and Management Research (ICSEMR)*. Chennai-India. https://doi.org/10.1109/ICSEMR.2014.7043606

López, I., Quintana, C. E., Ruiz, J. J., Peragón, F. C., & Dorado, M. P. (2014). Effect of the use of olive-pomace oil biodiesel/diesel fuel blends in a compression ignition engine: Preliminary exergy analysis. *Energy Conversion and Management*, *85*, 227–233. https://doi.org/10.1016/j.enconman.2014.05.084

Mawatari, T., Fukuda, R., Mori, H., Mia, S., & Ohno, N. (2013). High pressure rheology of environmentally friendly. *Tribology Letters*, *51*(2), 273–280. https://doi.org/10.1007/s11249-013-0180-4

Oommen, L. P., & Kumar, G. N. (2020). Influence of magneto-combustion on regulated emissions of an automotive engine under variable speed operation. *International Journal of Vehicle Structures and Systems*, *12*(1), 109–112. https://doi.org/10.4273/ijvss.12.1.25

Patel, P. M., Rathod, G. P., & Patel, T. M. (2014). Effect of magnetic field on performance and emission of single cylinder four stroke diesel engine. In *International organization of Scientific Research*, *4*(5), 28–34. *https://doi.org/10.9790/3021-04552834*

Perdana, D., Adiwidodo, S., Choifin, M., & Winarko, W. A. (2021). The effect of magnetic field variations in a mixture of coconut oil and jatropha on flame stability and characteristics on the premixed combustion. *EUREKA, Physics and Engineering*, *2021*(5), 13–22. https://doi.org/10.21303/2461-4262.2021.001996

Perdana, D., Adiwidodo, S., Subagyo, & Winarko, W. A. (2022). The role of perforated plate and orientation of the magnetic fields on coconut oil premixed combustion. *INMATEH - Agricultural Engineering*, *67*(2), 77–84. https://doi.org/10.35633/inmateh-67-07

Perdana, D., Yuliati, L., Hamidi, N., & Wardana, I. N. G. (2020). The role of magnetic field orientation in vegetable oil premixed combustion. *Journal of Combustion*, *2020*, 1–11. https://doi.org/10.1155/2020/2145353

Serrano, C., Portero, H., & Monedero, E. (2013). Pine chips combustion in a 50 KW domestic biomass boiler. *Fuel*, *111*, 564–573. https://doi.org/10.1016/j.fuel.2013.02.068

Shah, P. R., & Ganesh, A. (2018). A novel strategy of periodic dosing of soy-lecithin as additive during long term test of diesel engine fueled with straight vegetable oil. *Fuel*, *228*, 405–417. https://doi.org/10.1016/j.fuel.2018.04.121

Shan, F., Lin, Q., Zhou, K., Wu, Y., Fu, W., Zhang, P., et al. (2017). An experimental study of ignition and combustion of single biomass pellets in air and oxy-fuel. *Fuel*, *188*, 277–284. https://doi.org/10.1016/j.fuel.2016.09.069

Sree, S. N., Kumar, K. S., & Nidumolu, P. (2017). Experimental investigation on CI engine fuelled with the blends of olive oil methyl ester and diesel. *International Journal of Mechanical Engineering and Technology*, *8*(7), 125–132. http://iaeme.com/Home/issue/IJMET?Volume=8&Issue=7

Villot, C., Howard, M. E., & Kittredge, K. W. (2019). Comparison of various feedstocks for the microwave-assisted synthesis of biodiesel. *American Journal of Organic Chemistry*, *9*(2), 25–27. https://doi.org/10.5923/j.ajoc.20190902.01

Volpato, C. E. S., Do, A., Conde, P., Barbosa, J. A., & Salvador, N. (2012). Performance of cycle diesel engine using biodiesel of olive oil (B100). *Ciência e Agrotecnologia*, *36*(3), 348–353. https://doi.org/10.1590/S1413-70542012000300011.

Wahhab, H. A. A., Al-Kayiem, H. H., Aziz, A. A. R., & Nasif, M. S. (2017). Survey of invest fuel magnetization in developing internal combustion engine characteristics. *Renewable and Sustainable Energy Reviews*, *79*, 1392–1399. https://doi.org/10.1016/j.rser.2017.05.121